JOURNAL OF SOLID STATE CHEMISTRY 15, 261–270 (1975)

Electrical Transport Properties of Zn Doped ZnO

K. I. HAGEMARK AND L. C. CHACKA

3M Central Research Laboratories, Box 33221, St. Paul, Minnesota 55133

Received October 7, 1974

Electrical resistivity and Hall effect measurements at 77–373°K are presented for Zn doped ZnO crystals. The crystals have been doped systematically at 600–1100°C in controlled pressures of Zn. The concentration of electrons at room temperature is in the range $n_{RT} = 2.5 \times 10^{16}$ to 3.6×10^{18} cm^{-3}. The donor level E_D and the concentrations of donors N_D and acceptors N_A have been calculated from a best fit to the experimental relationships $\log n$ versus $1/T$ and $\log \mu_H$ versus $\log T$. At dilute concentrations of donors, two donor levels have been observed, $E_D{}^I = 0.043$–0.045 eV and a deeper level E_D^{II} greater than 0.165 eV. The ZnO was found to behave as a metal at $N_D \sim 6 \times 10^{18}$ cm^{-3}.

At least two different donors have to be assumed in order to explain the experimental results. It is suggested that interstitial Zn is the electrical active donor at higher doping levels. The nature of the other donor is not clear. Neither $1s^1$ H-type nor $1s^2$ He-type donors seem to explain all the observations consistently.

I. Introduction

Previous studies (*1–13*) of pure and doped ZnO single crystals have shown that native defects have an important influence on the electrical transport properties. Pure ZnO has been found to be an n-type semiconductor with resistivity ρ varying from about 0.04 ohm = cm (degenerate semiconductor) to about 10^6 ohm = cm or higher (highly compensated). Since this means that the physical properties of ZnO will vary over a large range, there is a need for controlling the concentration of the native defects. Also it is desirable to determine the nature of the native donor responsible for the n-type behavior.

Despite the numerous studies of ZnO, no systematic study has been conducted on the relationship between low-temperature electrical transport measurements and high-temperature doping conditions. In the present paper, we will discuss the electrical properties at 77–373°K of ZnO crystals systematically Zn-doped at high temperatures. By means of these data we can prescribe the proper vapor pressure of Zn and the doping temperature T needed to obtain desired electrical properties at lower temperatures.

The nature of the native donor responsible for the n-type behavior is still not very well understood. It is not expected that the electrical transport properties alone will provide all the insight needed in this matter. A combination of many techniques, epr, optical studies, etc., on the same crystals would be needed. The electrical properties, however, are very sensitive to the concentration of the defects. Two methods will be used to calculate the concentration of donor N_D and acceptors, N_A.

First, from the relationship of the concentration of conduction electrons n and T we can, by using a nonlinear least-squares method to the scaled data, determine N_D, N_A, donor level with respect to conduction band E_D and the spin degeneracy β of the donor. The n-type behavior of pure ZnO comes from excess Zn incorporated either as interstitial Zn_i or oxygen vacancy V_O. In either case a two electron $1s^2$ or helium-type donor is expected

Copyright © 1975 by Academic Press, Inc.
All rights of reproduction in any form reserved.
Printed in Great Britain

with $\beta = 0.5$. In several earlier studies (*1–13*), however, the electrical transport data have been explained assuming a single electron donor, $1s^1$ or hydrogen-type with $\beta = 2$. It will be shown that certain observations favor a $1s^1$-type while other observations favor a $1s^2$-type donor.

Secondly, from the electron mobility data, subtracting out the scattering effects not due to defects, we have calculated N_D and N_A. The latter results are compared with the results from the first method.

II. Experimental

A. Electrical Measurements

A conventional Hall method similar to the one described by Rupprecht (*4*) was used. Details of the method are described elsewhere (*14*). The ZnO crystals were fabricated into rectangular shaped bars with dimensions $2 \times 2 \times 15$ mm. Low resistance ohmic indium contacts were formed by "sparking" (capacitor discharge welding). The measurements were taken from 77–373°K with the magnetic induction B at 10 kG.

B. Doping Experiments

The 3 *M* vapor phase grown crystals were used. Emission spectrographic and mass spectrographic analyses show no major impurities above 1 ppma except for Si (10–20 ppma). The stoichiometric composition of ZnO crystals was changed by high-temperature treatments at controlled pressures of zinc. A sealed silica ampoule with a ZnO crystal at one end and a piece of metallic Zn at the other end was heated in a two temperature zone furnace. The vapor pressure of zinc (*15*) is given by

$$p_{Zn} = 1.66 \times 10^5 \exp(-1.22/kT_{Zn})(\text{atm}) \quad (1)$$

where $k = 0.8617 \times 10^{-4}$ eV degree^{-1} and T_{Zn} is temperature of Zn metal. In these type of doping experiments the upper limit of p_{Zn} is determined by the fact that T_{Zn} cannot exceed the temperature of ZnO, T_{ZnO}, to avoid transport of Zn to the ZnO side. Furthermore, T_{Zn} must be chosen high enough to create a back pressure of Zn to prevent excessive sublimation of ZnO to the Zn metal side of the ampoule. To obtain lower pressures of zinc, the crystals were heated in Ar gas at 1 atm (where $p_{Zn} = 2p_{O_2}$) and in O_2 gas at 1 atm. In these cases the zinc pressure is calculated from (*16*)

$$p_{Zn} \times p_{O_2}{}^{1/2} = K_{ZnO} = 1.5 \times 10^{10} \exp(-4.89/kT)(\text{atm})^{3/2}. \quad (2)$$

The time of equilibration varied from 2 days for $T_{ZnO} = 1100$°C to two weeks for $T_{ZnO} = 700$°C. After the heat treatment the crystals were rapidly cooled to room temperature in less than 1 min. To minimize the surface effects, the crystals were etched for 8–10 min in hot (85–90°C) concentrated H_3PO_4 before the electrical properties were measured. The etch removed about 50 μm from the surface. Emission spectrographic and mass spectrographic analyses (approximately 1 ppm sensitivity) indicated that the impurity content did not change during the heat treatment.

III. Results

In three sets of doping experiments T_{ZnO} was kept constant at 1000, 800, and 700°C while T_{Zn} was varied from T_{ZnO} down to 400°C in steps of 100°C; crystals were also heated in pure argon and oxygen gas at 1 atm. In addition, saturated zinc doping experiments were performed at 1100, 900, and 600°C.

The electron concentration n is calculated from

$$n = -\frac{r}{e \cdot R_H} \quad (3)$$

where r is assumed equal to $3\pi/8$, e is the elementary charge, and R_H is the measured Hall coefficient.

In Figs. 1 and 2 the results at 1100°C are shown as $\log n$ versus $1/T$ (°K) and $\log \mu_H$ versus $\log T$. The doping conditions are given for each set of data. The first number refers to T_{ZnO} and the second number to T_{Zn}. When T_{Zn} equalled T_{ZnO} or when Ar and O_2 were used, only one temperature is given.

From Fig. 1 it is obvious that n increases and from Fig. 2 that μ_H decreases with

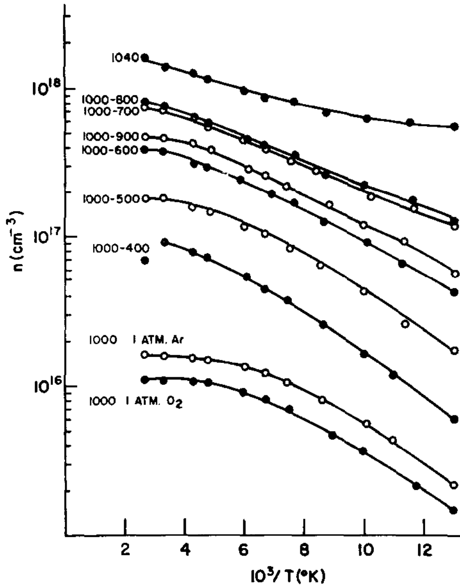

FIG. 1. The concentration of conduction electron n is shown versus $10^3/T$ for the 1000°C series. The first number refers to T_{ZnO}, the second number to T_{Zn} at the high-temperature treatment.

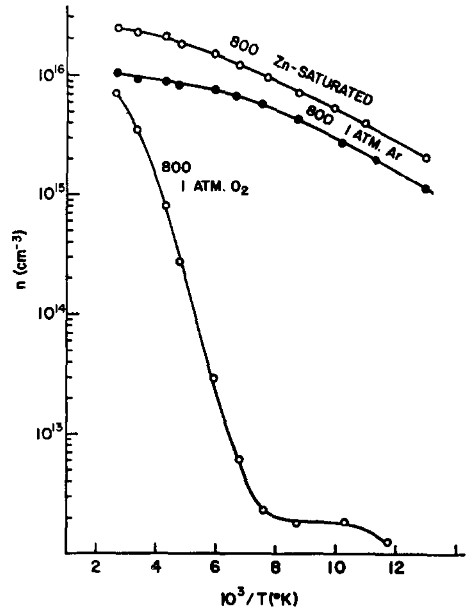

FIG. 3. The concentration of conduction electron n is shown versus $10^3/T$ for the 800°C series. The steeper slope for the 1 atm O_2 case indicates a deeper donor is involved ($E_D > 0.165$ eV).

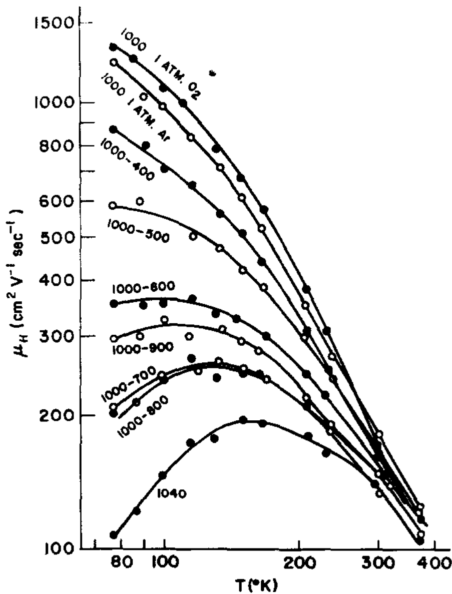

FIG. 2. The Hall mobility μ_H is shown versus $\log T$ for the 1000°C series.

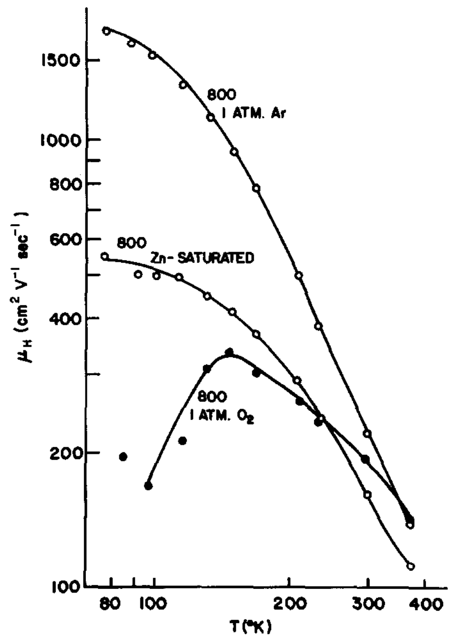

FIG. 4. The Hall mobility μ_H is shown versus $\log T$ for the 800°C series. The shape of the curve at the lower temperature for the 1 atm O_2 case suggests another conduction mechanism is becoming important.

increasing p_{Zn}. Thus we conclude that native donors are introduced with increasing p_{Zn}. The run at 1000–900 shows an unexplained

deviation from the trend. However, more runs should be made to check the significance of this deviation.

In Figs. 3 and 4 are shown $\log n$ versus $1/T$ (°K) and $\log \mu_H$ versus $\log T$ at 800°C for the Zn saturated condition and for Ar and O_2 at 1 atm. The results at 800–1atm O_2 differ considerably from the results at the other doping conditions. The steeper slope of $\log n$ versus $1/T$ (°K) in Fig. 3 indicates that a deeper donor is involved. This is illustrated in Fig. 5 where the Fermi level, with respect to the conduction band E_F, versus $1/T$ (°K) is shown (see Eq. (6) for calculation E_F). In this case, the Fermi level in the intermediate temperature range seems to be pinned at a donor level about 0.165 eV below the conduction band. In the other doping experiments the donor level is less than 0.05 eV. The rapid decrease of μ_H at lower temperatures in the case of 800–1 atm O_2, is also distinctly different from the behavior of the other crystals.

In Fig. 6, the concentration of electrons at room temperature n_{RT} is shown as $\log n_{RT}$ versus $\log p_{Zn}$ (atm) at constant $T_{ZnO} = 1000$, 800, and 700°C. Dashed lines are drawn through the points. The slope of $\log n_{RT}$ versus $\log p_{Zn}$ at constant T is close to 1/3. As shall be discussed later, this indicates that a doubly ionized donor is involved. At lower p_{Zn} ($\log p_{Zn}$ in the range −5 to −10) the electron concentration is constant, indicating the presence of a second donor with concentration about 2×10^{16} cm^{-3}. The Zn saturated data at 1100, 900, and 600 are also shown in Fig. 6. The solid line represents the Zn saturated results and can in the range 600–1100°C be expressed as

$$n = 2.68 \times 10^{21} \exp(-0.83 \text{ eV}/kT) \text{ cm}^{-3}.$$

This compares fairly well with results by Scharowsky (*6*) and Thomas (*5*) (400–750°C)

$$n = 2.68 \times 10^{20} \exp(-0.65 \text{ eV}/kT) \text{ cm}^{-3}.$$

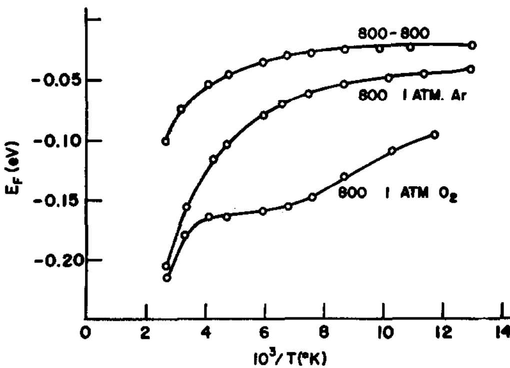

FIG. 5. The Fermi level with respect to conduction band as function of $10^3/T$ for the 800°C series. A deeper donor is clearly involved in the 1 atm O_2 case.

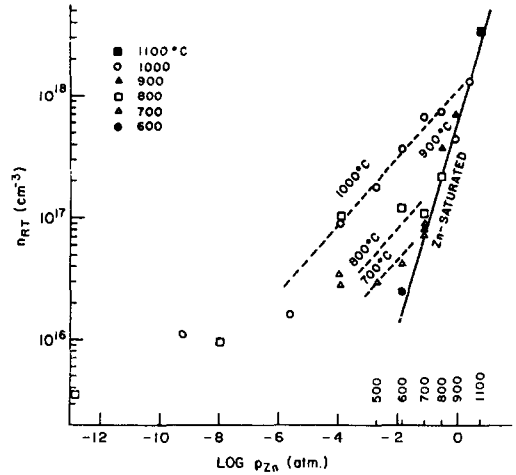

FIG. 6. The concentration of conduction electrons n_{RT} as function of the zinc pressure at the high-temperature doping conditions.

Another point of interest is the change in color of the crystals from clear to light yellow ($n_{RT} \sim 4 \times 10^{17}$ cm^{-3}) to reddish brown to deep red with increasing Zn in the crystals. The color change is due to a shift in the absorption edge and has been discussed by Scharowsky (*6*).

IV. Discussion

Both n and μ_H give information about the point defects. In the discussion we will use the $\log n$ versus $1/T$ to obtain the donor level E_D, the concentration of donors N_D and acceptors N_A. Then we will employ plots of $\log \mu_H$ versus $\log T$ to obtain the concentration of ionized and neutral scattering centers. For a consistent fit the results for N_D and N_A from the $\log n$ versus $1/T$ and $\log \mu_H$ versus $\log T$ should be in agreement.

A. Electron Concentration n

For a semiconductor with a concentration of one type of donor N_D and a total concentration of acceptors N_A, the electron concentration is given by (*17*)

$$n + N_A = N_D[1 + \beta \exp(\varepsilon_D + \eta)]^{-1} \quad (4)$$

where β is related to the spin degeneracy factor for the donor level; $\beta = 2$ for $1s^1$-type donor, $\beta = 0.5$ for $1s^2$-type donor; $\varepsilon_D = E_D/kT$, $\eta = E_F/kT$ where E_F is the Fermi level with respect to the conduction band.

For $\eta < 1.3$, Blakemore (*18*) has shown the Fermi level is given by

$$E_F = kT \log\left[\frac{N_C}{n} - 0.27\right]^{-1} \text{eV} \quad (5)$$

where the density of states in the conduction band

$$N_C = 4.83 \times 10^{15} \left(\frac{m^N}{m}\right)^{3/2} T^{3/2} \quad (6)$$

and m^N is the density of states mass. The present calculations are valid for $\eta < 1.3$ or $n/N_C < 1.84$.

From Eq. (4), a theoretical value n_{th} for the electron concentration may be calculated from

$$n_{\text{th}} = -\frac{2c}{b + (b^2 - 4ac)^{1/2}} \quad (7)$$

where

$$a = 1 - 0.27\frac{1}{\beta}\exp(-\varepsilon_D).$$

$$b = N_A + \frac{1}{\beta}(N_C + 0.27(N_D - N_A))\exp(-\varepsilon_D).$$

$$c = -\frac{1}{\beta}N_C(N_D - N_A)\exp(-\varepsilon_D).$$

The values for the four parameters N_D, N_A, E_D, and β, leading to a best fit, were found by minimizing the standard deviation of the normalized data

$$\sigma_N = \left[\frac{1}{M}\Sigma\left(1 - \frac{n_{\text{th}}}{n}\right)^2\right]^{\frac{1}{2}}$$

where M is the number of data points.

A nonlinear least-squares method was used to determine N_D, N_A, and E_D for the two choice of β, $\beta = 2$ or $\beta = 0.5$. We have assumed $m^N/m = 0.3$ for ZnO (*38*). The results for the 1000°C series are given in Table I. It appears that $\beta = 0.5$ (helium-type donor) gives a slightly better fit (lower values of σ_N). But because of the uncertainty in the value of the density-of-states mass, the simplicity of our model, and the uncertainty in the experimental data, the difference is not considered significant enough to discriminate between $\beta = 2$ or 0.5.

In Fig. 7 the E_D, as determined by the best-fit method, is shown as a function of $N_D^{1/3}$ for $\beta = 2$ where

$$E_D = 0.045 - 2.8 \times 10^{-8} N_D^{1/3} \text{ eV} \quad (8)$$

and $E_D \sim 0$ for $N_D = 4 \times 10^{18}$ cm^{-3}. A similar relation can be obtained for $\beta = 0.5$

$$E_D = 0.043 - 2.4 \times 10^{-8} N_D^{1/3} \text{ eV} \quad (9)$$

and $E_D \sim 0$ for $N_D = 6 \times 10^{18}$ cm^{-3}. The inverse of $N_D^{1/3}$ may be considered as the average distance between the donors. Thus, E_D, due to overlap of donor wave functions, is expected to decrease with increasing N_D. According to Pearson and Bardeen (*19*)

$$\frac{\partial E_D}{\partial N_D^{1/3}} = -3 \times 10^{-8} \quad (10)$$

which is very close to what we find in Eqs. (8) and (9). However, the significance of these relations is still not completely understood (*20*).

According to our data, the thermal E_D at dilute donor concentration is about 0.043 to 0.045 eV and Zn doped ZnO becomes metallic ($E_D = 0$) at $N_D = 4$ to 6×10^{18} cm^{-3} (average donor distance 55–60 Å). These values are only slightly different from $E_D = 0.051$ eV and $N_D = 6 \times 10^{18}$ cm^{-3} reported by Hutson (*3*).

B. Hall Mobility μ_H

We will calculate the Hall mobility and by a best fit to the experimental data obtain the concentration of donors and acceptors. These values will be compared to the values obtained from the log$n$ versus $1/T$ fit.

TABLE I
RESULTS FROM CARRIER CONCENTRATION ANALYSIS, EQUATION (7), AND HALL MOBILITY ANALYSIS, EQUATION (18)

	Carrier-concentration analysis					Hall mobility analysis	
Doping	β	σ	E_D (meV)	N_D (cm^{-3})	N_A (cm^{-3})	N_D (cm^{-3})	N_A (cm^{-3})
1000	2	3.26×10^{-2}	1.0	2.92×10^{18}	2.03×10^{17}		
	0.5	4.24×10^{-2}	0.5	3.54×10^{18}	1.61×10^{18}	2.10×10^{18}	5.20×10^{17}
1000–950	2	5.40×10^{-2}	16.0	1.33×10^{18}	1.68×10^{17}		
	0.5	1.98×10^{-2}	14.5	1.76×10^{18}	9.11×10^{17}	1.16×10^{18}	1.73×10^{17}
1000–900	2	7.51×10^{-2}	17.5	9.60×10^{17}	1.59×10^{17}		
	0.5	3.48×10^{-2}	19.0	1.08×10^{18}	4.93×10^{17}	9.29×10^{17}	7.90×10^{16}
1000–800	2	4.44×10^{-2}	13.5	1.60×10^{18}	1.87×10^{17}		
	0.5	3.55×10^{-2}	9.5	2.80×10^{18}	1.70×10^{18}	1.17×10^{18}	2.63×10^{17}
1000–700	2	5.19×10^{-2}	14.0	1.52×10^{18}	1.94×10^{17}		
	0.5	3.54×10^{-2}	11.0	2.42×10^{18}	1.41×10^{18}	1.13×10^{18}	2.39×10^{17}
1000–600	2	5.50×10^{-2}	19.5	7.30×10^{17}	1.31×10^{17}		
	0.5	1.67×10^{-2}	18.5	1.09×10^{18}	6.27×10^{17}	7.48×10^{17}	5.38×10^{16}
1000–500	2	5.61×10^{-2}	23.5	3.29×10^{17}	8.29×10^{16}		
	0.5	2.71×10^{-2}	21.5	6.84×10^{17}	4.72×10^{17}	3.89×10^{17}	1.31×10^{16}
1000–400	2	1.27×10^{-2}	23.5	2.61×10^{17}	1.42×10^{17}		
	0.5	1.02×10^{-2}	21.0	9.25×10^{17}	8.09×10^{17}	1.88×10^{17}	3.67×10^{15}
1000–1 atm Ar	2	1.19×10^{-2}	37.0	2.16×10^{16}	4.72×10^{15}		
	0.5	1.40×10^{-2}	25.5	1.74×10^{17}	1.57×10^{17}	—	—
1000–1 atm O_2	2	2.11×10^{-2}	46.5	1.16×10^{16}	1.84×10^{14}		
	0.5	3.35×10^{-2}	23.0	2.60×10^{17}	2.48×10^{17}	—	—

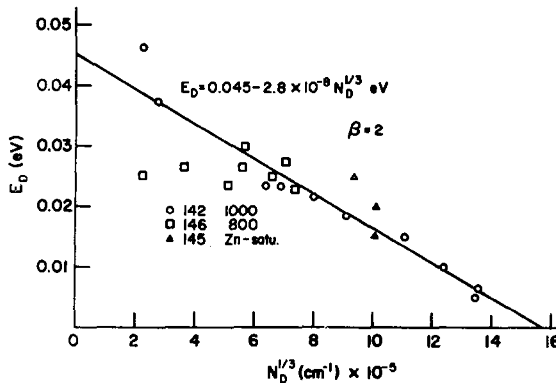

FIG. 7. The donor level E_D is shown versus $N_D^{1/3}$. A H-type donor ($\beta = 2$) is assumed.

The mobility of electrons is related to the scattering mechanisms. The following types of scattering processes will be considered:

(i) lattice: optical, acoustical, and piezoelectric mode;

(ii) defects: ionized and neutral defect scattering.

The latter two mechanisms are related to the concentration of defects and are of the most interest in the present discussion.

The expressions for the various lattice mobilities have been derived by theoretical considerations and, to a certain extent, by a best fit to experimental Hall mobility at

higher temperatures where defect mode scattering becomes negligible.

1. Optical mode scattering. According to Devlin (*21*), the optical mode Hall mobility is

$$\mu_{HLO} = r_{HLO}\,\phi\mu_F \tag{11}$$

where

$$\mu_F = \frac{e}{2\alpha\omega_o m^x}\left[\exp\left(\frac{\hbar\omega_o}{kT}\right) - 1\right]$$

and the polaron coupling constant α is

$$\left(\frac{1}{\varepsilon_\infty} - \frac{1}{\varepsilon_s}\right)\left(\frac{m^x}{m}\right)^{1/2}\left(\frac{E_H}{\hbar\omega_o}\right)^{1/2};$$

ω_o is the angular frequency of the longitudinal optical phonons; m^x is the effective mass, different from the density-of-states mass discussed in the previous section; ϕ is a slow varying function of the temperature and r_{HLO} is the Hall coefficient factor for optical mode scattering. The latter two functions have been computed by Devlin (*21*); ε_∞ and ε_s is the high frequency and static dielectric constant and $E_H = 13.6$ eV. By choosing $\hbar\omega_o = 72.5$ meV (*22*), $m^x = 0.27m$ (*23*), $\varepsilon_\infty = 3.75$ (*22*), and $\varepsilon_s = 8.75$ (*22*), both parallel to the c-axis, we get

$$\mu_H = r_{HLO}\,\phi 27.4[\exp(841/T) - 1]. \tag{12}$$

In the temperature range considered here we have assumed $r_{HLO}\cdot\phi \approx 1$ without too much error (*21*).

2. Acoustical mode scattering. According to Bardeen and Shockley (*24*) the acoustical lattice mode Hall mobility is given by

$$\mu_{HLA} = \frac{3\pi}{8}\frac{(8\pi)^{1/2}\hbar^4 C_{ll}\,e}{3E_{ln}^2 m^{x5/2}(kT)^{3/2}} \tag{13}$$

where C_{ll} is the average longitudinal elastic constant and equal to 2.1×10^{12} dyn cm^{-2} (*22*); E_{ln} is the shift of the edge of conduction band per unit dilation (deformation potential); $\mu_H/\mu = 3\pi/8$ for acoustical mode scattering and $m^x = 0.27m$ (*23*). From a best fit to the experimental data, we find

$$\mu_{HLA} = 3.02 \times 10^6 \cdot T^{-3/2}\ \text{cm}^2\ \text{V}^{-1}\ \text{sec}^{-1}$$

leading to $E_{ln} = 31.2$ eV (in agreement with *1*). Although a high value, similar high values have been reported for other II–VI compounds by Rode (*25*).

3. Piezoelectric mode scattering. The piezoelectric mode mobility has been discussed by Zook (*26*). Parallel to c-axis he reported

$$\mu_{LP}^{\parallel} = 3160\left(\frac{m}{m^x}\right)^{3/2} T^{-1/2}\ \text{cm}^2\ \text{V}^{-1}\ \text{sec}^{-1} \tag{14}$$

and perpendicular to c-axis $\mu_{LP}^{\perp} = 2.8\ \mu_{LP}^{\perp}$. The Hall coefficient factor is assumed to be unity.

4. Ionized defect scattering. The Brooks–Herring expression (*27*) for the ionized defect scattering mobility μ_{HI} is

$$\mu_{HI} = r_{HI}\frac{2^{7/2}\,\varepsilon_r^2(kT)^{3/2}}{\pi^{3/2}e^3 m^{x1/2}g(b)}\frac{1}{N_I} \tag{15}$$

where

$$g(b) = \ln(1+b) - \frac{1}{1+b}$$

$$b = \frac{6\varepsilon_r m^x(kT)^2}{\pi e^2\hbar^2 n^x}$$

and screening charge

$$n^x = N_C \times \mathscr{F}_{-1/2}(\eta) \tag{16}$$

The Fermi–Dirac integrals

$$\mathscr{F}_j(\eta) = \frac{1}{\Gamma(j+1)}\int_0^\infty \frac{\varepsilon^j\,d\varepsilon}{\exp(\varepsilon - \eta) + 1}$$

have been tabulated by Blakemore (*28*). The Hall coefficient factor r_{HI} is given by Beer (*29*) to be

$$r_{HI} = \frac{315\pi}{512}\left[\frac{g(b)}{g(3b/2)}\right]^2$$

and the concentration of ionized centers is $N_I = n + 2N_A$.

In the Brook–Herring expression for the screening charge the charged donors and acceptors were also considered. (n^x in Eq. (13) is then $n^x = n + (n + N_A)(1 - (n + N_A)/N_D)$.) We have found it more consistent to consider the screening by electrons only (see Dingle (*30*) and Mansfield (*31*)). As long as the defects are far enough apart, i.e., outside the screening radius R (*30*) of the screened coulombic scattering center, $R = 9.923 \times 10^{-8}\ \varepsilon_r T^{-1/4}(m^x/m)^{-3/4}[\mathscr{F}_{-1/2}(\eta)]^{-1/2}$, this should be a better approximation. In ZnO the shortest

distance between the donors will be along the *a* directions. For a donor concentration of 4.21×10^{17} cm^{-3} or 10 ppma, this corresponds to an average distance of 150 Å between the scattering centers. For an equivalent concentration of electrons (all donors ionized in an uncompensated crystal) the screening radius R is only 31 Å at $T = 77$°K. For $n = N_D/10$, R is 86 Å or approximately only half of the average distance between the donors. For compensated crystals, of course, one can no longer neglect the effect of donors and acceptors. But in that case one no longer has independent scattering from individual scattering centers either.

By choosing the average value $\varepsilon_r = 8.5$, we find

$$\mu_{HI} = r_{HI} \frac{4.57 \times 10^{17} T^{3/2}}{g(b)} \frac{1}{N_I}$$

where $b = 2.96 \times 10^{14} T^2 (1/n^x)$.

5. *Neutral defect scattering.* The mobility related to the scattering by neutral defects is given by Erginsoy (*32*) to be

$$\mu_N = 1.44 \times 10^{22} \left(\frac{m^x}{m}\right) \frac{1}{\varepsilon_r N_N} \tag{17}$$

where the concentration of neutral defects is $N_N = N_D - (n + N_A)$, assuming no other neutral defects are present. The Hall coefficient factor is assumed to be unity.

6. *The calculated Hall mobility.* Because the acoustical scattering mode is not the only important scattering mode we have assumed the theoretical Hall mobility to be

$$\frac{1}{\mu_H} \approx \frac{1}{\mu_{HL}} + \frac{1}{\mu_{HI}} + \frac{1}{\mu_{HN}} \tag{18}$$

where the lattice Hall mobility is calculated from

$$\frac{1}{\mu_{HL}} \approx \frac{1}{\mu_{HLO}} + \frac{1}{\mu_{HLA}} + \frac{1}{\mu_{HLP}}. \tag{19}$$

The values for N_D and N_A obtained from the best fit are given in Table I and compare favorably to the values from the log$n$ versus $1/T$ fit for $\beta = 2$ ($1s^1$-type donor). In general the value obtained for N_A from the mobility fit is lower than the one from conduction electron analysis.

At the higher doping levels (close to degeneracy at 77°K) the agreement is not as good. As discussed in (*33*), the donor band conduction mechanism becomes important at the lower temperatures and at a higher concentration of donors.

A similar good fit has been obtained for the 800°C doping series except for the 800°C 1 atm O_2 run. In this case, a deeper donor becomes the electrical active donor. At low temperature the electron concentration becomes very low, the crystal is practically compensated, with the possibility of doubly ionized scattering centers or donor band conduction.

C. Type of Native Donor

From Fig. 6, logn_{RT} versus logp_{Zn}, it appears that at least two donors are present. At higher doping levels, $n_{RT} > 10^{16}$ cm^{-3} or $p_{Zn} > 10^{-4}$ atm, the electrical properties are controlled by a native donor. At the intermediate doping levels, $p_{Zn} < 10^{-4}$ atm, another donor dominates. Since the concentration of this donor (about 1 ppma) does not change significantly with p_{Zn}, the donor could be due to an impurity or a frozen-in native donor.

We will discuss what the electrical transport property measurements indicate with respect to the nature of the two donors. From the measurements the following facts point to a $1s^1$ H-type donor.

1. The donor level $E_D = 0.045$ eV is in good agreement with the value calculated from a scaled $1s^1$ H-type donor level

$$E_H = 13.6 \frac{m^x/m}{\varepsilon_r^2} \approx 0.05 \text{ eV}$$

A scaled $1s^2$ He-type donor level (Hylleraas (*34*))

$$E_{He} = \frac{me^4}{2\hbar^2} \frac{m^x}{m} \frac{1}{\varepsilon_r^2} \times \left[Z^2 - \tfrac{5}{4}Z + 0.31488 - \frac{0.01752}{Z} + \frac{0.00548}{Z^2}\right]$$

$$= 24.58 \frac{m^x}{m} \frac{1}{\varepsilon_r^2} = 0.902 \text{ eV}$$

where Z is charge of the nuclei (in this case equal to 2). Thus, E_{He} is too large for what is observed.

2. The most consistent fit between the results from $\log n \approx 1/T$ and from $\log \mu$ versus $\log T$ is obtained for $\beta = 2$, or a $1s^1$-type donor.

Several points, however, favor a $1s^2$ He-type donor.

1. If excess Zn is incorporated as either interstitial zinc Zn_i or oxygen vacancies V_O, the donor should in either case have two available electrons and consequently $\beta = 0.5$. However, a crystal field splitting of the levels might occur.

2. At higher temperature and higher doping levels (1000°C series) the relation $\log n \sim 1/3 \log p_{Zn}$ is indicative of a doubly ionized donor, in agreement with other II–VI measurements. (See, for example, Smith (*35*).)

3. A slightly better fit is obtained for $\beta = 0.5$ for the $\log n$ versus $1/T$ curve at higher doping levels.

4. The deeper donor level $E_D > 0.165$ eV for crystal No. 146G is consistent with the second ionization energy of a $1s^2$ He-type donor.

$$E_D = Z^2\, 13.6\, \frac{m^x/m}{\varepsilon_r^{\,2}} \approx 0.20 \text{ eV}.$$

Unfortunately, none of these observations are conclusive with respect to the nature of the donor. However, from the comments made with respect to the relationship $\log n$ versus $\log p_{Zn}$ we speculate that the native donor at higher doping levels is related to interstitial zinc, Zn_i. At lower doping levels the other donor could very possibly be related to a frozen-in oxygen vacancy V_O. The concentration of V_O would be determined by the conditions during the crystal growth at high temperatures. Since all ZnO crystals used in the present study were originally grown under the same conditions, it is reasonable to assume that all the crystals would have a similar concentration of frozen-in V_O. Our speculations are consistent with the diffusion data by Moore and Williams (*36*). They found Zn_i diffuses much more rapidly than V_O in the temperature range considered in the present study. However, Hoffman and Lauder (*37*) question the result by Moore and Williams. More data seem to be needed to clear up this controversy.

V. Summary

Electrical resistivity and Hall effect data at 77–373°K have been presented for Zn doped ZnO single crystals. The crystals have been doped systematically at 600–1100°C in controlled pressures of Zn and the electrical transport properties are related to the thermodynamic variables p_{Zn} and T. By means of the data we can prescribe the proper vapor pressure of Zn and the doping temperature T needed to obtain desired electrical properties at lower temperatures.

From a best fit for the $\log n$ versus $1/T$ curve and the $\log \mu$ versus $\log T$ curve, we have calculated the concentration of donors and acceptors, and the donor level E_D. At dilute donor concentrations, $N_D < 10^{17}$ cm^{-3}, two donor levels have been observed, $E_D = 0.043$ to 0.045 eV and $E_D > 0.165$ eV. Consistent with earlier observations, ZnO is found to become metallic at $N_D \approx 6 \times 10^{18}$ cm^{-3}. Also, at least two different donors have to be assumed in order to explain the results. One of the donors is suggested to be related to interstitial zinc Zn_i and the other one to be a frozen-in oxygen vacancy V_O.

The nature of the donors has not been pinpointed. According to the electrical transport property results neither $1s^1$ H- nor $1s^2$ He-type donors seem acceptable. It is possible that crystal field splitting of the donor level has to be considered.

VI. Acknowledgments

The authors wish to acknowledge the assistance of E. L. Cook and G. K. Lindeberg in the computer programming.

References

1. P. Wagner and R. Helbig, *J. Phys. Chem. Solids* **35**, 327 (1974).
2. G. Bogner, *J. Phys. Chem. Solids* **19**, 235 (1961).
3. A. R. Hutson, *Phys. Rev.* **108**, 222 (1957).
4. H. Rupprecht, *J. Phys. Chem. Solids* **6**, 144 (1958).
5. D. G. Thomas, *J. Phys. Chem. Solids* **3**, 229 (1957).
6. E. Scharowsky, *Z. Physik* **135**, 318 (1953).
7. D. G. Thomas and J. J. Lander, *J. Chem. Phys.* **25**, 1136 (1956).

8. E. Mollwo, *Z. Physik* **138**, 478 (1954).
9. J. J. Lander, *J. Phys. Chem. Solids* **15**, 324 (1960).
10. G. Bogner and E. Mollwo, *J. Phys. Chem. Solids* **6**, 136 (1958).
11. D. G. Thomas, *J. Phys. Chem. Solids* **9**, 31 (1958).
12. A. Hausmann and W. Teuerle, *Z. Physik* **257**, 299 (1972).
13. A. Hausmann and W. Teuerle, *Z. Physik* **259**, 189 (1973).
14. F. J. McFadden and K. I. Hagemark, 3M Research Report (1970).
15. "Handbook for Chemistry and Physics," 50th ed., p. D-145, The Chemical Rubber Company, Cleveland (1969–1970).
16. F. A. Kröger, "The Chemistry of Imperfect Crystals," p. 694, North-Holland, Amsterdam (1964).
17. J. S. Blakemore, "Semiconductor Statistics," p. 133, Pergamon, New York (1962).
18. J. S. Blakemore, "Semiconductor Statistics," p. 360, Pergamon, New York (1962).
19. G. L. Pearson and J. Bardeen, *Phys. Rev.* **75**, 865 (1949).
20. J. S. Blakemore, "Semiconductor Statistics," p. 166, Pergamon, New York (1962).
21. S. S. Devlin *in* "Physics and Chemistry of II–VI Compounds," M. Aven and J. S. Prener (Eds.), p. 560, North-Holland, Amsterdam (1967).
22. M. Neuberger, "II–VI Semiconducting Compounds Data Tables," EPIC, Hughes Aircraft Company, Culver City (1969).
23. A. R. Hutson, *J. Phys. Chem. Solids* **8**, 467 (1959).
24. J. Bardeen and W. Schockley, *Phys. Rev.* **80**, 72 (1950).
25. D. L. Rode, *Phys. Rev.* **B2**, 4036 (1970).
26. J. D. Zook, *Phys. Rev.* **136A**, 869 (1964).
27. H. Brooks, *Advan. Electronics and Electron Phys.* 7, 158 (1955).
28. J. S. Blakemore, "Semiconductor Statistics," p. 346, Pergamon, New York (1962).
29. A. C. Beer *in Solid State Physics*, Supplement 4, F. Seitz and D. Turnbull (Eds.), p. 128, Academic Press, New York (1963).
30. R. B. Dingle, *Phil. Mag.* **46**, 831 (1955).
31. R. Mansfield, *Proc. Phys. Soc.* (London) **B69**, 76 (1956).
32. C. Erginsoy, *Phys. Rev.* **79**, 1013 (1950).
33. P. W. Li and K. I. Hagemark, *J. Solid State Chem.* **12**, 371 (1975).
34. E. A. Hylleraas, *Z. Physik* **65**, 209 (1930).
35. F. J. T. Smith, *Solid State Comm.* **8**, 263 (1970).
36. W. J. Moore and E. L. Williams, *Disc. Farad. Soc.* **28**, 86 (1959).
37. J. W. Hoffman and I. Lauder, *Trans. Farad. Soc.* **66**, 2346 (1970).
38. A. R. Hutson, *J. Appl. Phys.* **32**, 2287 (1961).